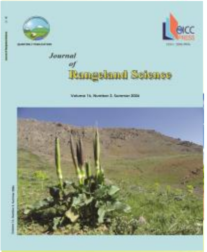

J. Rangeland Sci., 2026; 16(3): 256-265

Journal of Rangeland Science (JRS)

https://doi.org/10.57647/JRS.2026.1603.23

Research Article

Estimation of Chlorophyll Content and Leaf Area Index of Vegetation Cover Using Remote Sensing in Malayer Rangeland, Iran

Behnaz Attaeian[1,*], Mahnaz Mohammadi[1], Behrooz Mohammadparast[2]

[1] *Faculty of Natural Resources and Environment, Malayer University, Malayer, Iran*
[2] *Faculty of Science, Malayer University, Malayer, Iran*

*Corresponding author: b.attaeian@malayeru.ac.ir

Article History:

Received:
28 August 2025

Revised:
05 December 2025

Accepted:
29 December 2025

Published in Issue:
30 September 2026

Abstract

Accurate estimation of plant biophysical and biochemical parameters is essential for sustainable rangeland management. This study aimed to investigate the potential of Landsat 8 satellite imagery in estimating LAI and chlorophyll content of mountain rangeland species in Malayer, Iran. Field sampling was conducted on May 23, 2016. Forty plots, each corresponding to the 30×30 m spatial resolution of Landsat pixels, were selected. Within each plot, five 1 m^2 subplots were sampled, resulting in 200 plant samples. LAI was measured using a WINAREA-UT-10 leaf area meter, and chlorophyll content was determined by the Arnon method using spectrophotometric analysis. A cloud-free Landsat 8 image dated May 1, 2016, was preprocessed to calculate vegetation indices and extract reflectance values from various spectral bands. Among the tested indices, the Chlorophyll Index green (CI Green) had a strong correlation with measured chlorophyll content ($r=0.61$, $p<0.01$). Similarly, the LAI index showed a significant correlation with field-measured LAI ($r = 0.63$, $p < 0.01$). Regression models showed that CI and the short-wavelength infrared (SWIR band) were included in the final regression model, with positive and negative effects, respectively. These variables explained 42% of the total variance in the field-measured chlorophyll content, while the LAI index explained 36% of the variation in field-measured LAI. Other indices, such as Normalized Difference Vegetation Index (NDVI), Difference Vegetation Index (DVI), Soil Adjusted Vegetation Index (SAVI), Transformed Soil Adjusted Vegetation Index (TSAVI), and Ratio Vegetation Index (RVI) showed weak or non-significant correlations with both variables. These results indicate that CI Green and LAI are more reliable indices than conventional vegetation indices for evaluating plant biochemical and structural properties in semi-arid, mountainous rangelands. The findings confirm the potential of remote sensing techniques, especially CI and LAI indices, for cost-effective and scalable vegetation monitoring in semi-arid rangelands.

Keywords: Biodiversity Ecological Monitoring, Plant Biophysical Traits, Spectral Indices, Landsat 8 Imagery, Semi-arid Ecosystems

Cite this article: Attaeian , B., Mohammadi, M. & Mohammadparast, B., (2026). Estimation of Chlorophyll Content and Leaf Area Index of Vegetation Cover Using Remote Sensing in Malayer Rangeland, Iran, *Journal of Rangeland Science,* 16(3), 255-265.
https://doi.org/10.57647/jrs.2026.1603.23

1. Introduction

Rangelands are among the most extensive anthropogenic landscapes on earth and the livelihood of almost 500 million people depends on it (Eddy et al., 2017). For the optimal utilization of rangeland services, accurate assessment of plant characteristics is essential. Biophysical measurements of plant species are particularly important because they sustain rangeland functioning throughout their life cycle. Among these, the leaf area index (LAI) defined as the projected leaf area per unit ground surface area (Liu et al., 2007) is one of the most critical vegetation biophysical variables. LAI is widely used to evaluate the structural characteristics of plant communities (Andalibi et al., 2022) and strongly influences photosynthesis, transpiration, energy balance, and overall plant health in ecological systems (Turner et al., 1999). Plant species with higher LAI can intercept more precipitation, reduce soil erosion and runoff, and sustain higher primary productivity, thereby enhancing ecosystem resilience to global change and disturbance. Although direct methods for measuring LAI are labor-intensive and time-consuming, they provide reliable estimates and are commonly used to validate indirect methods (Yan et al., 2019). Although LAI and chlorophyll content often covary in rangeland vegetation (Daughtry et al., 2000), they represent distinct biophysical attributes and are estimated through their respective structural and pigment-related spectral responses. Both variables are key indicators of vegetation condition, productivity, and overall ecosystem functioning.

Chlorophyll, an essential plant pigment, plays a central role in photosynthesis and is closely linked to plant growth and nutrient uptake (Kolluru et al., 2023). Quantifying the temporal dynamics of chlorophyll is therefore critical for monitoring plant physiological status and primary production (Jay et al., 2017). Variations in chlorophyll content provide insights into plant stress, developmental stage, and overall health, making it a key parameter in remote sensing applications (Kolluru et al., 2023). Direct measurements of canopy chlorophyll and LAI are relatively accurate but are time-consuming and costly. Although less precise, indirect approaches such as vegetation indices are particularly valuable in rangeland ecosystems, where field sampling is often difficult or infeasible. The application of remote sensing technology, particularly in the red-edge region of the electromagnetic spectrum, has proven effective for estimating key indicators of vegetation health (Pei et al., 2018). This approach uses satellite and aerial imagery to monitor large rangeland areas over time, enabling the detection of changes in chlorophyll content and LAI without extensive field sampling (Taugourdeau et al., 2014; Kumar et al., 2022). The red-edge region, located between the red and near-infrared bands, is highly sensitive to vegetation properties such as chlorophyll concentration and leaf structure (Wong et al., 2013; Taugourdeau et al., 2014; Pei et al., 2018). This sensitivity enhances the discrimination of vegetation types, supporting accurate mapping of heterogeneous landscapes and effective habitat management. Importantly, it enables the early detection of vegetation stress before visible symptoms appear, allowing timely interventions across ecosystems (Tsalyuk et al., 2015). Satellite-based measurements in the red-edge region also facilitate large-scale, long-term monitoring of vegetation dynamics, providing valuable data on ecosystem responses to environmental change (Taugourdeau et al., 2014; Tsalyuk et al., 2015). Hyperspectral imagery yields fine-scale insights at local levels, while ground-based measurements provide high-resolution data that complement satellite and airborne observations. A common remote-sensing approach for estimating LAI and chlorophyll content is to establish physical relationships between these variables and vegetation indices (VIs) derived from visible, Near-infrared (VNIR), and short-wave infrared (SWIR) bands, such as the enhanced vegetation index (EVI), soil-adjusted vegetation index (SAVI), and normalized difference vegetation index (NDVI) (Fadl et al., 2024). Multispectral and hyperspectral indices greatly improve the monitoring of ecosystem health and the detection of changes in vegetation biophysical properties. VIs derived from imagery provide consistent empirical measures of vegetation, allowing inferences about biophysical conditions and temporal dynamics across landscapes (Eddy et al., 2017). Traditionally, LAI estimation has relied on spectral vegetation indices derived from red (R) and Near InfraRed (NIR) reflectance values (Qi et al., 2000). Although these indices are widely applied, many saturate at high LAI levels, reducing accuracy (Behifar et al., 2023). Recent studies demonstrate the potential of advanced indices and modeling approaches. For example, Solgi et al. (2023) found species-specific chlorophyll distribution patterns in *Acacia* and *Sycamore*, while Behifar et al. (2023) reported that EVI, using non-linear regression, provided superior LAI estimates in silage maize. Remote sensing techniques increasingly overcome the limitations of field measurements by offering accurate, repeatable, and spatially extensive assessments of parameters such as leaf area, biomass, chlorophyll, and nitrogen (Ma et al., 2012). A multisensor evaluation in Ardabil Province, Iran, confirmed the spatiotemporal variability of LAI across plant functional types, with Sentinel-2B outperforming other sensors due to its high resolution and strong correlation with ground-based measurements (Andalibi et al., 2022). In forest ecosystems, Brown et al. (2019) reported that the Invertible Forest Reflectance Model (INFORM) outperformed SNAP L2B in estimating both LAI and canopy chlorophyll content (CCC) from Sentinel-2 MSI data. INFORM achieved higher accuracy in reproducing observed spectra, indicating its suitability for forest applications. More broadly, remote sensing has proven effective for monitoring natural ecosystems, including rangelands, owing to its cost-efficiency and extensive spatial coverage (Murugan et al., 2016). Vegetation indices are central to such analyses, with reported accuracies including chlorophyll retrieval at a relative root mean square deviation (RMSD) of 19% and LAI estimation with $r^2 = 0.85$ in rangeland ecosystems (Houborg et al., 2015).

Mountainous rangeland ecosystems are ecologically diverse and provide critical services such as erosion control, water regulation, and habitat for native flora and fauna. These environments are defined by steep terrain, shallow soils, and variable climatic conditions, which strongly influence plant community composition and structure. The study area, located in the mountainous rangelands of western Iran. It is the habitat a variety of resilient plant genera, including *Stipa* (Poaceae), *Astragalus* (Fabaceae), *Artemisia* (Asteraceae), *Onopordon* (Asteraceae), and *Alyssum* (Brassicaceae) (Fattahi et al., 2021). Each genus exhibits distinct morphological and physiological traits that promote survival in semi-arid, nutrient-poor conditions. For example, species of *Astragalus* typically develop deep taproots to access subsurface water, while members of *Onopordon* possess spiny leaves and a rosette growth form that reduce herbivory and water loss (Asri, 2011). *Artemisia* is characterized by small, silver-gray leaves covered with trichomes that reflect sunlight and reduce transpiration (Asri, 2011). These adaptations make members of this genus valuable indicators for monitoring vegetation dynamics and assessing the health of mountainous rangelands. Their sensitivity to environmental stressors underscores the importance of accurate and scalable monitoring techniques, such as remote sensing, for sustainable rangeland management. The SardKooh mountainous rangeland in Malayer County, Iran, represents a vulnerable semi-arid ecosystem that provides essential services such as soil and water regulation, forage production, and habitat for native flora. However, its steep terrain, quick seasonal changes, and limited access hinder traditional monitoring, emphasizing the need for scalable methods to find long-term solutions. This study investigates the potential of Landsat 8 satellite imagery for estimating leaf area index (LAI) and chlorophyll content in native rangeland species by addressing this gap through evaluating the performance of spectral indices. The findings provide efficient, cost-effective tools for ecological monitoring and support evidence-based management of fragile mountainous ecosystems. This study aims to evaluate the potential of Landsat 8 imagery and vegetation spectral indices for estimating leaf area index (LAI) and chlorophyll content in semiarid mountain ecosystems, thereby addressing the critical need for non-destructive monitoring of vegetation health in these environment.

2. Materials and methods

2.1. Study area

The study area, SardKooh Mountain, is located in Malayer, Hamadan Province, western Iran, between 48°51′00″E and 48°53′24″E longitude and 34°15′00″N and 34°16′12″N latitude (Fig 1). SardKooh Mountain has an altitude of 2777 m above sea level. The region has a semi-arid climate with an average annual precipitation of 315 mm and an evapotranspiration of 2665 mm, and the study area encompasses about 853 ha on its southern piedmont. Vegetation surveys in the study area identified a total of 167 species belonging to 24 families and 114 genera, with the families Leguminosae and Compositae representing the highest species richness (Fattahi et al., 2021). The predominant plant genera in the study area include *Astragalus*, *Artemisia*, *Stipa*, *Onosma*, and *Centaurea*, along with several other taxa characteristic of semi-arid rangelands (Table 1). A total of 28 rangeland plant species belonging to nine families is listed in Table 1. The family Compositae (Asteraceae) is the most species-rich with 9 species, followed by Leguminosae (Fabaceae) with 5 species. Boraginaceae and Poaceae each include two and three species, respectively. The remaining families – Amaryllidaceae, Apiaceae, and Caryophyllaceae – each comprise two species, while Lamiaceae and Rosaceae each contain a single species. The dominant Asteraceae family often exhibits xeromorphic drought-tolerance traits to minimize water loss and enhance water uptake.

2.2. Sampling method

To determine sampling points, a false color composite (FCC) of a Landsat 8 image (R = 5, G = 4, B = 3) was generated, as this combination provides optimal discrimination of vegetation from other surface features. A total of 40 sampling points were selected, with plots established at the exact dimensions of a Landsat pixel (30 × 30 m) to improve calculation accuracy. Within each plot, aboveground biomass was sampled from five 1 m² subplots by harvesting and weighing all plants. Fresh leaf and stem samples were then weighed in the field using a laboratory scale (Citizen Scale, CY360, Netherlands).

2.3. LAI field measurement

To measure LAI, five fresh, fully expanded leaves from the aboveground samples in each plot were selected and weighed. Leaf area was determined using a WINAREA-UT-10 device, and the mean LAI of the five leaves was calculated. A ratio was then established between total fresh leaf weight, average LAI, and the total fresh biomass of each plot to estimate plot-level LAI (Pandey and Singh, 2011).

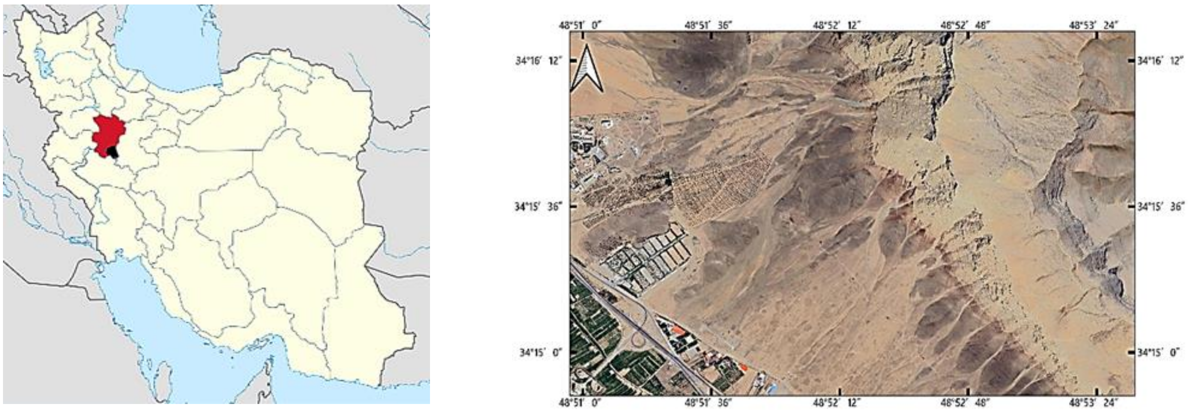

Figure 1. Map and geographic coordinates of the study area, located 4 km southeast of Malayer city, Iran

Table 1. Major rangeland species of the study area according to Flora Iranica

No.	Family	Species
1	Amaryllidaceae	*Allium atroviolaceum* Boiss. *Allium scabriscapum* Boiss.
2	Apiaceae	*Echinophora platyloba* DC. *Ferula ovina* Boiss.
3	Boraginaceae	*Onosma chrysochaeta* Bornm. *Onosma kotschyi* Boiss.
4	Brassicaceae	*Alyssum lanigerum DC.*
5	Caryophyllaceae	*Acanthophyllum microcephalum* Boiss. *Dianthus orientalis* Adams
6	Asteraceae	*Artemisia fragrans Willd.* *Centaurea aucheri* DC. *Centaurea persica* Boiss. *Centaurea virgata* Lam. *Cousinia pichleriana* Bornm. *Echinops ecbatanus* Bornm. ex Rech.f. *Onopordum leptolepis* DC. *Taraxacum officinale* F.H.Wigg. *Xeranthemum longepapposum* Fisch. & C.A.Mey.
7	Lamiaceae	*Stachys inflata* Benth.
8	Fabaceae	*Astragalus brachyodontus* Boiss. *Astragalus effusus* Bunge *Astragalus parrowianus* Boiss. & Hausskn. *Astragalus tribuloides* Delile *Trifolium repens* L.
9	Poaceae	*Bromus tectorum* L. *Poa bulbosa* L. *Stipa barbata* Desf.
10	Rosaceae	*Amygdalus lycioides* Spach

Table 2. The formula for different calculated vegetation indices

No	Vegetation Index	Abrev.	Equation	Reference
1	Normalized Difference Vegetation Index	NDVI	$NIR - R/NIR + R$	(Rouse et al., 1974)
2	Divergence Vegetation Index	DVI	$NIR - R$	(Tucker, 1979)
3	Weighted Divergence Vegetation Index	WDVI	$NIR - s, R$	(Clevers, 1989)
4	Soil Adjusted Vegetation Index	SAVI	$(1 + l)NIR - R/NIR + R + L$	(Huete, 1988)
5	Transformed Soil Adjusted Vegetation Index	TSAVI	$\frac{s, (NIR - s \times R - a)}{(a, NIR + R - as + X \times (1 + s^2))}$	(Baret and Guyot, 1991)
6	Ratio Vegetation Index	RVI	NIR/R	(Nagler et al., 2005)
7	Brightness Index	BI	$\sqrt{R^2 + NIR^2}$	(Dehni and Lounis, 2012)
8	Leaf Area Index	LAI	$-(\frac{\ln(0,69 - SAVI)/0,59)}{0,91})$	(Allen et al., 2009)
9	Chlorophyll Index Green	CI Green	$(\frac{NIR}{Green}) - 1$	(Gitelson et al., 2003)

*NIR: Near Infrared; R: Red; S: Slope of soil equation; A: Intercept of soil equation; L: Empirical correction factor

10.57647/jrs.2026.1603.23

Table 3. Descriptive statistics of field-measured chlorophyll contents and Leaf Area Index

Variables	Maximum	Minimum	Mean	Standard deviation
Chlorophyll a (mg.g^{-1},FW)	1.24	0.43	0.82	0.21
Chlorophyll b (mg.g^{-1},FW)	0.44	0.06	0.22	0.09
Total chlorophyll (mg.g^{-1},FW)	1.69	0.50	1.05	0.30
Leaf area index	2.59	1.12	1.64	0.25

Table 4. Correlation between both field-measured total chlorophyll content and Leaf Area Index, with spectral bands and vegetation indices

Spectral Indices	Abrev.	Total chlorophyll	Leaf Area Index
Ratio Vegetation Index	RVI	0.19	-0.01
Soil Adjusted Vegetation Index	SAVI	0.19	-0.01
Transformed Soil Adjusted Vegetation Index	TSAVI	0.13	0.01
Weighted Divergence Vegetation Index	WDVI	0.12	-0.05
Normalized Difference Vegetation Index	NDVI	0.19	-0.01
Divergence Vegetation Index	DVI	0.19	-0.04
Chlorophyll index Green	CI Green	0.61*	-
LAI	LAI index	-	0.63*
Brightness Index	BI	-0.06	-0.04
Coastal Aerosol Band	Coastal	-0.09	-0.03
Blue spectral bands	Blue	0.27	0.07
Green spectral bands	Green	0.09	0.06
Red spectral bands	Red	-0.14	0.03
Near infrared reflectance	NIR	-0.12	-0.10
Short-wave infrared	SWIR	-0.43*	0.10

*significant at 0.05 level

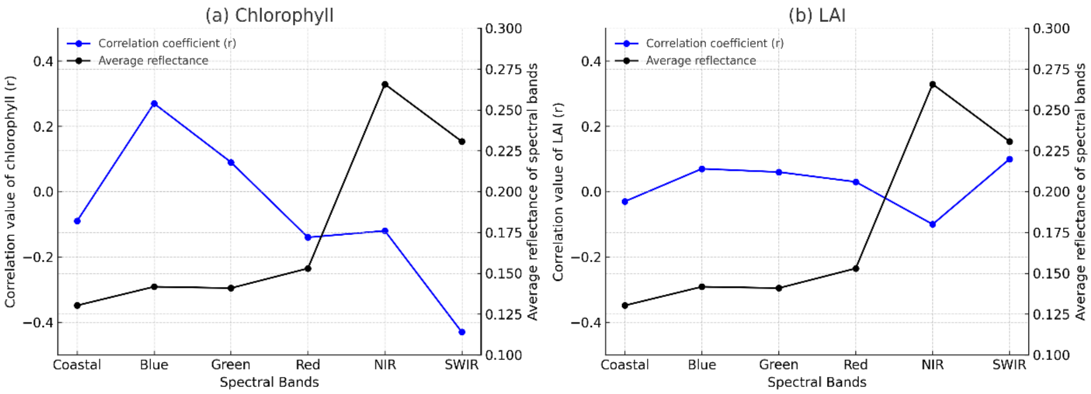

Figure 2. a) Correlation trends between chlorophyll content and average values of spectral bands, and b) correlation trend between LAI with the average values of spectral bands

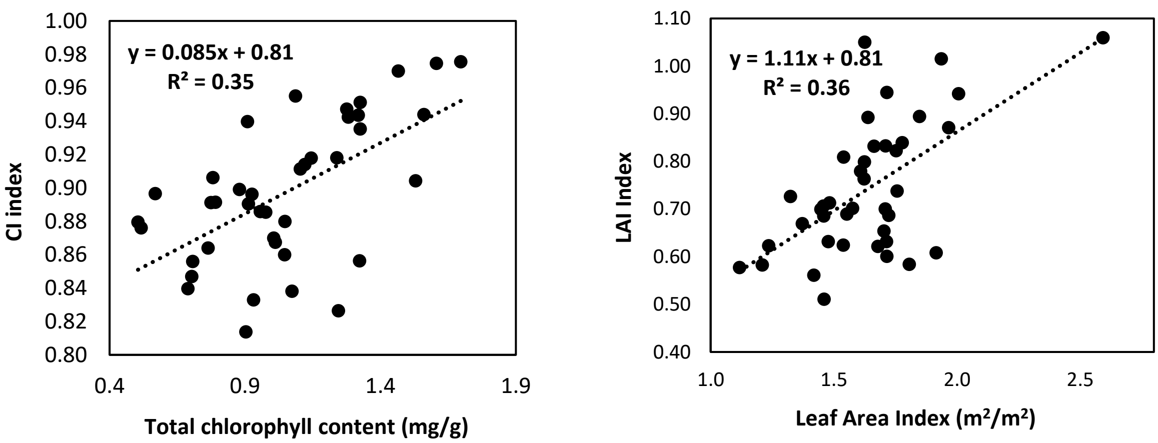

Figure 3. Linear regression between vegetation indices (CI and LAI) and corresponding field measurements

10.57647/jrs.2026.1603.23

Table 5. Multiple linear regression analysis was used to predict chlorophyll content, and simple linear regression was used to predict LAI values using spectral bands and vegetation indices as independent variables

Field variables (Y)	Vegetation index (X)	Regression Coefficients (b)	R^2	P value
Chlorophyll content	CI Green and SWIR	$Chl = 3.58CI - 6.65SWIR$	0.42	0.01
LAI	LAI Index	$LAI = 0.81 + 1.11LAI\ Index$	0.36	0.01

SWIR=short-wavelength infrared
CI Green=Chlorophyll index green

2.4. Chlorophyll content measurement

To measure the chlorophyll content of rangeland species, plant samples were identified and transferred to the laboratory for chemical analysis. Chlorophyll concentration was determined following the Arnon method (Arnon, 1949).

The optical density of the extracts was recorded using a spectrophotometer (Hitachi U-2800) at 646.8 nm and 663.2 nm to estimate chlorophyll *a* and chlorophyll *b*, respectively. The instrument was calibrated with 80% acetone as the blank.

2.5. Remotely sensed data

Landsat 8 OLI-TIRS imagery dated 1 May 2016 was obtained from the USGS database for this study. Before analysis, standard preprocessing steps, including radiometric and geometric corrections, were performed in ENVI v5.3 to ensure accurate calculations. Subsequently, several spectral indices were derived, including NDVI, DVI, WDVI, RVI, SAVI, TSAVI, BI, and LAI (Table 2). Field sampling data were then integrated into ArcGIS v10.3 based on the geographic coordinates of the sampling plots to extract the corresponding digital number (DN) values from the spectral images.

2.6. Statistical analysis

All statistical analyses were performed using SAS v9.3 software. Pearson correlation coefficients were calculated to assess the strength and direction of relationships between spectral indices and field-measured variables, including chlorophyll content and LAI. Linear regression models were then developed to quantify these relationships and evaluate the predictive performance of selected vegetation indices.

In the regression equations, field-measured chlorophyll content and LAI were treated as dependent variables (Y), while the vegetation indices and spectral band values derived from Landsat 8 imagery served as independent variables (X).

The general form of the regression model was expressed as Y = aX + b, where Y is the measured biophysical variable, X is the spectral index, a and b are regression coefficients. Model performance was evaluated using the coefficient of determination (R^2), root mean square error (RMSE), and T, F, and p-values to determine goodness of fit and statistical significance.

3. Result

3.1. Descriptive statistics of chlorophyll contents and Leaf Area Index

Descriptive statistics of field-measured chlorophyll values and LAI is presented in Table 3. Result showed that chlorophyll a content across the 40 plots ranged from 0.43 to 1.24 $mg.g^{-1}$FW with a mean of 0.82 $mg.g^{-1}$ and a standard deviation (SD) of 0.21 $mg.g^{-1}$. Similarly, chlorophyll b values ranged from 0.06 to 0.44 $mg.g^{-1}$ (mean = 0.22 $mg.g^{-1}$, SD = 0.09 $mg.g^{-1}$), while total chlorophyll content ranged from 0.50 to 1.69 $mg.g^{-1}$ (mean =1.05 $mg.g^{-1}$, SD = 0.30 $mg.g^{-1}$). These findings indicate considerable variation in pigment content among the sampled plants' fresh weight.

Descriptive statistics for the field-measured LAI across the 40 plots (Table 3) revealed a mean LAI of 1.64 (SD =0.25), with values ranging from 1.12 to 2.59 leaf area (m^2)/ground area (m^2).

3.2. Relationship between chlorophyll contents and spectral indices

The correlation between total chlorophyll content and various spectral indices is summarized in Table 4. The Chlorophyll Index (CI) exhibited a positive and significant correlation with field chlorophyll content (r = 0.61, p<0.05). This pattern was visually confirmed in Fig 3, where CI values increased with higher chlorophyll content across the plots. It should be noted that chlorophyll values were normalized (z-score transformation) before correlation analysis and plotting. Although the relationship between the two variables was significant (p <0.05), the data in Fig 3 were scattered. In contrast, SWIR band reflectance showed a moderate negative correlation with total chlorophyll content (r = –0.43, p<0.05), which indicated the higher SWIR reflectance values were associated with lower chlorophyll levels. It is likely due to the inverse relationship between leaf water status or structure and chlorophyll absorption in that spectral region. No significant correlations were observed between chlorophyll content and the other vegetation indices tested (NDVI, DVI, SAVI, TSAVI, RVI, WDVI, BI) or with the other spectral bands (Coastal, Blue, Green, Red, NIR) (p>0.05) (Table 4 and Fig 2). To predict field-measured chlorophyll content, a multiple linear regression model was developed using both CI and

SWIR as independent variables. The resulting model equation was:

$$Chlorophyll\ (mg.g^{-1}) = 3.58 \times CI - 6.65 \times SWI \qquad (1)$$

Where:
SWIR short-wavelength infrared
CI=Chlorophyll index green

As shown in Table 5, the multiple regression model that included both CI and SWIR explained 42% of the total variance in measured chlorophyll content ($R^2 = 0.42$, $F = 22.17$, $p < 0.01$). Both predictor variables were statistically significant, and coupled with low values of RMSE, provided a reasonably accurate estimation of total chlorophyll content in mountainous rangelands using Landsat 8 data. A simple regression between chlorophyll content and CI was also developed. Fig 3 visually showed the relationship between the two variables.

3.3. Relationship between leaf area index and spectral indices

The correlation between measured LAI with nine Landsat 8–8-derived indices and individual spectral bands is presented in Table 4 and Fig 2. The Chlorophyll Index Green (CI Green) exhibited a positive and significant correlation with field LAI ($r = 0.63$, $p<0.05$). All other indices (NDVI, DVI, WDVI, RVI, SAVI, TSAVI, BI) and spectral bands (Coastal, Blue, Green, Red, NIR, SWIR) had no significant correlations with field LAI ($p>0.05$), indicating the suitability of the Chlorophyll Index Green (CI Green) for estimating structural LAI in these sparse vegetation communities. A simple linear regression for the estimation of measured LAI as (y) on the LAI index as (x) was fitted (Table 5, Fig 3), as follows:

$$\mathrm{LAI} = 0.81 + 1.11\mathrm{LAI\ index}, \qquad (2)$$

Where: R^2=0.36, explained 36% of the total variation in measured LAI in the field. The F value was significant ($p<0.01$), confirming the model's overall significance. RMSE = 0.17, indicating relatively low average prediction error given the small magnitude of LAI values. In Fig 3, the positive slope of the regression line confirmed the above model. Among all tested spectral metrics, the Chlorophyll Index Green (CI Green) consistently outperformed conventional vegetation indices and individual bands in estimating canopy leaf area in semi-arid mountainous rangelands. Its moderate correlation (r =0.63) and substantial (R^2=0.36) demonstrated that even a single well-tuned index can provide significant, spatially continuous estimates of LAI for ecosystem monitoring.

1. Discussion

This study demonstrated that targeted spectral metrics outperformed generic greenness indices for estimating plant biochemical and structural properties in a semi-arid rangeland. Among the tested variables, the Green Chlorophyll Index (CI) showed the strongest relationship with measured chlorophyll (r=0.61), and combining CI with SWIR further improved chlorophyll prediction using multiple regression (R^2=0.42). In contrast, conventional broadband indices (e.g., NDVI and related red–NIR ratios) exhibited weak and often non-significant associations with chlorophyll and LAI under low-biomass, soil-exposed conditions. For canopy structure, a Landsat-derived LAI index achieved a significant correlation with field-measured LAI ($r = 0.63$). Collectively, these findings indicated that indices designed to reduce soil background effects and avoid early saturation are more reliable for sparse canopies than widely used red–NIR vegetation indices. The superior behavior of CI was consistent with criteria proposed for an optimal chlorophyll-sensitive vegetation index: strong sensitivity without rapid saturation, minimal soil background contamination, robustness to canopy structure, stability across sensors, and limited susceptibility to atmospheric and geometric effects (Bannari and Staenz, 2016). CI leverages the green region around the chlorophyll absorption features and thus maintains sensitivity where red–NIR indices tend to saturate. Our results also showed that adding SWIR contributes complementary information, plausibly tied to leaf water/structure and background moisture, which can modulate canopy optical properties and reduce unexplained variance in chlorophyll estimates (Clevers et al., 2017). At the same time, the incremental gain from SWIR was modest and consistent with SWIR's sensitivity to soil moisture and mixed-pixel effects in semi-arid scenes, suggesting that CI captures the primary biochemical signal, while SWIR refines predictions by accounting for structural and moisture differences (Gitelson et al., 2003; Clevers et al., 2017). In contrast, the limited performance of NDVI and related red–NIR metrics in our site aligns with well-known constraints under sparse canopies as rapid saturation of the red–NIR contrast and strong sensitivity to soil brightness, litter, and shadowing (Qi et al., 2000; Daughtry et al., 2000).

In our plots, characterized by low leaf area and patchy cover, soil background dominated much of the signal, decoupling NDVI from chlorophyll and LAI dynamics. This was consistent with recent observations that, although NDVI remains widely used, it can under-represent vegetation variability in arid and semi-arid ecosystems (Pei et al., 2018; Kizilgeci et al., 2021; Fadl et al., 2024). These results reinforce the need to deploy indices less sensitive to soil background and with greater biochemical specificity when monitoring vegetation function in drylands (Gitelson et al., 2003; Houborg et al., 2015). Sensor characteristics further explain performance differences. Our Landsat-based analysis necessarily aggregated plot measurements to 30-m pixels, introducing spatial averaging and mixed-pixel effects that can weaken field–satellite relationships (Turner et al., 1999). Studies using Sentinel-2, with higher spatial resolution and red-edge bands, often report stronger retrievals of chlorophyll and LAI in similar environments (Andalibi et al., 2022; Yan et al., 2019). This agrees with our finding that CI and an LAI index outperform generic indices on Landsat, while also pointing to the potential gains from sensors with red-edge information and finer spatial detail (Houborg et al., 2015; Andalibi et al., 2022). Several methodological factors influenced our results.

First, the dynamic range of vegetation was limited (semi-arid, low biomass), which inherently constrains index–variable correlations even for well-targeted indices (Behifar et al., 2023). Second, scale mismatch between plot-scale measurements (~1 m^2) and 30-m satellite pixels introduced aggregation errors and increased noise (Turner et al., 1999; Sebastiani et al., 2023). Third, a temporal offset existed between image acquisition and field sampling, which can be consequential in seasonally dynamic, water-limited systems (Tsalyuk et al., 2015). Future efforts could mitigate these issues by synchronizing field campaigns with satellite overpasses, exploiting time-series approaches to interpolate conditions on the sampling date, and/or integrating higher-resolution platforms (e.g., UAVs) to improve plot–pixel comparability (Dreier et al., 2025; Jay et al., 2017; Eddy et al., 2017). Finally, beyond index selection and sensor choice, modeling strategy matters. Incorporating multi-band features (visible–NIR–SWIR) and using robust, interpretable models can capture complementary biochemical and structural information while controlling for soil/background variability (Clevers et al., 2017; Houborg et al., 2015; Kolluru et al., 2023). Emerging machine learning and hybrid physical-statistical approaches offer promising routes to improve retrievals in heterogeneous, low-cover rangelands, if models are properly validated with field data and uncertainty is reported (Sebastiani et al., 2023).

In summary, CI (for chlorophyll) and a soil-adjusted LAI index (for canopy structure) provided the most reliable estimates in our semi-arid rangeland, whereas red–NIR greenness metrics (e.g., NDVI) were inadequate under low-cover, soil-exposed conditions. Practical implications include prioritizing chlorophyll-sensitive, soil-robust indices and, where possible, higher-resolution/red-edge sensors to improve monitoring of vegetation function and drought responses. Addressing scale and timing issues, and leveraging multi-band or advanced modeling frameworks, can further enhance operational mapping of chlorophyll and LAI, supporting more informed rangeland management in water-limited environments (Bannari and Staenz, 2016; Gitelson et al., 2003; Clevers et al., 2017; Andalibi et al., 2022; Turner et al., 1999).

5. Conclusion

This study demonstrated the challenges and opportunities of remote sensing for quantifying chlorophyll content and LAI in semi-arid, sparsely vegetated rangeland. Traditional red–NIR vegetation indices, including NDVI and EVI, exhibited low sensitivity and rapid saturation under low-biomass conditions, limiting their effectiveness. In contrast, the Green Chlorophyll Index (CI) and a combined CI + SWIR model provided more robust and stable chlorophyll estimations, while a specialized Landsat-derived LAI index showed a moderate yet statistically significant correlation with field-measured LAI. These findings underscore the importance of using tailored and physiologically relevant spectral indices that minimize soil-background effects and saturation, particularly in ecosystems with sparse canopies and heterogeneous soil conditions. Furthermore, the outcomes confirmed that improving sensor characteristics, such as incorporating red-edge or SWIR bands and employing finer spatial resolutions, can substantially enhance retrieval accuracy and interpretation of vegetation dynamics in semi-arid systems. Temporal synchronization between field sampling and image acquisition, as well as the integration of multi-temporal datasets, also emerges as a key factor influencing model performance and reliability. Incorporating higher-resolution imagery from UAV platforms and leveraging multi-temporal satellite observations can therefore provide a stronger basis for accurate and scalable vegetation assessments. Future work should aim to combine these technical advancements with advanced analytical frameworks, including data fusion and machine learning, to overcome the remaining limitations of index-based vegetation modelling. Overall, this research provides a valuable methodological framework for improving vegetation monitoring and assessment in challenging semi-arid landscapes, thereby supporting more informed ecosystem management, restoration planning, and sustainable rangeland conservation.

Authors Contribution
Authors have contributed equally in preparing and writing the manuscript.

Availability of data and materials
The data that support the findings of this study are available on request from the corresponding author.

Conflict of interests
The authors have no conflicts/competing interests.

References

Allen, R.G. and Pereira, L.S., 2009. Estimating crop coefficients from fraction of ground cover and height. Irrigation Science, 28(1), pp.17-34

Andalibi. L., Ghorbani. A., Darvishzadeh. R., Moameri. M., Hazbavi. Z., Jafari. R. and Dadjou. F., 2022. Multisensor assessment of leaf area index across ecoregions of Ardabil Province, northwestern Iran. Remote Sensing, 14(22), pp. 5731. https://doi.org/10.3390/rs14225731

Arnon, D.I., 1949. Copper enzymes in isolated chloroplasts: Polyphenoloxidase in Beta vulgaris. Plant Physiology. 24(1), pp. 1–15. https://doi.org/10.1104/pp.24.1.1

Asri, Y., 2011. Plants of Iranian Rangelands, Vol. 2: Dicotyledons. RIFR Press, Tehran. 530 pp. eseed.rifr-ac.ir (in Persian)

Bannari, A. and Staenz, K., 2016. Hyperspectral chlorophyll indices sensitivity analysis to soil backgrounds in agricultural applications using field, Probe-1, and Hyperion data. Proceedings of the 2016 IEEE International Geoscience and Remote Sensing Symposium. (IGARSS), pp. 7129–7132. https://doi.org/10.1109/IGARSS.2016.7730860

Behifar, M., Aghighi, H., Matkan, A. and Salehi Shahrabi, H., 2023. Analysis of Sentinel-2 satellite images to estimate leaf area index of corn crops. Iranian Journal of Remote Sensing & GIS. 15(1), pp.1–15. (In Persian). https://doi.org/10.52547/gisj.15.1.1

Baret, F. and Guyot, G., 1991 Potentials and limits of vegetation indices for LAI and APAR assessment. Remote Sensing of Environment, 35, pp. 161–173. https://doi.org/10.1016/0034-4257(91)90009-U

Brown, L., Booker, A., Ogutu, O. and Jadunandan, D., 2019 Estimating forest leaf area index and canopy chlorophyll content with Sentinel-2: An evaluation of two hybrid retrieval algorithms. Remote Sensing, 11(15), pp.1752. https://doi.org/10.3390/rs11151752

Clevers, J.G., Kooistra, L. and Van den Brande, M.M., 2017. Using Sentinel-2 data for retrieving LAI and leaf and canopy chlorophyll content of a potato crop. Remote Sensing. 9(5), pp. 405. https://doi.org/10.3390/rs9050405

Clevers J.G.P.W. 1989. The derivation of the simplified reflectance model for the estimation of leaf area index. *Remote Sensing of Environment* 25:17–26. https://doi.org/10.1016/0034-4257(88)90041-7

Daughtry, C., Walthall, C.L., Kim, M.S., Brown, De Colstoun, E. and McMurtrey J.E. III., 2000. Estimating corn leaf chlorophyll concentration from leaf and canopy reflectance. Remote Sensing of Environment, 74(2), pp. 229–239. https://doi.org/10.1016/S0034-4257(00)00113-9

Dehni, A. and Lounis, M., 2012. Remote sensing techniques for salt-affected soil mapping: Application to the Oran region of Algeria. Procedia Engineering, 33, pp. 188–198. https://doi.org/10.1016/j.proeng.2012.01.1193

Dreier, A., Lopez, G., Bajracharya, R., Kuhlmann, H. and Klingbeil, L., 2025. Structural wheat trait estimation using UAV-based laser scanning data: Analysis of critical aspects and recommendations based on a case study. Precision Agriculture, 26(1), pp.18. https://doi.org/10.1007/s11119-024-10202-4

Eddy, I.M., Gergel, S.E., Coops, N.C., Henebry, M.G., Levine, J., Zerriffi, H. and Shibkov, E., 2017. Integrating remote sensing and local ecological knowledge to monitor rangeland dynamics. *Ecological Indicators* 82:106–116. https://doi.org/10.1016/j.ecolind.2017.06.033

Fattahi, B., Ghorbanpour Delivand, M., Gorgani, B. and Ghasemi Haji Abadi, F., 2021. Chorology, biological form and composition of species of plant elements in the southern slopes of the mountain ranges of Garmeh Malayer. Plant Ecology and Conservation, 9(18), pp. 267–285.

Fadl, M.E., AbdelRahman, M.A.E., El-Desoky, A.I. and Yasser, A.S., 2024. Assessing soil productivity potential in arid region using remote sensing vegetation indices. Journal of Arid Environments, 222, pp. 105166. https://doi.org/10.1016/j.jaridenv.2024.105166

Gitelson, A.A., Vina, A., Arkebauer, T.J., Rundquist, D.C., Keydan, G. and Leavitt, B., 2003. Remote estimation of leaf area index and green leaf biomass in maize canopies. Geophysical Research Letters, 30(5), pp. L08403. https://doi.org/10.1029/2002GL016450

Houborg, R., McCabe, M., Cescatti, A., Gao, F., Schull, M. and Gitelson, A., 2015. Joint leaf chlorophyll content and leaf area index retrieval from Landsat data using a regularized model inversion system (REGFLEC). Remote Sensing of Environment, 159, pp. 203–221. https://doi.org/10.1016/j.rse.2014.12.008

Huete, A.R., 1988. A soil-adjusted vegetation index (SAVI). Remote Sensing of Environment, 25, pp.295–309. https://doi.org/10.1016/0034-4257(88)90106-X

Jay, S., Gorretta, N., Morel, J., Maupas, F., Bendoula, R., Rabatel, G., Dutartre, D., Comar, A.and Baret, F., 2017. Estimating leaf chlorophyll content in sugar beet canopies using millimeter-to centimeter-scale reflectance imagery. Remote Sensing of Environment, 198, pp.173–186. https://doi.org/10.1016/j.rse.2017.06.008

Kizilgeci, F., Yildirim, M., Islam, M.S., Ratnasekera, D., Iqbal, M.A. and Sabagh, A.C., 2021. Normalized difference vegetation index and chlorophyll content for precision nitrogen management in durum wheat cultivars under semi-arid conditions. Sustainability, 13(7), pp. 3725. https://doi.org/10.3390/su13073725

Kolluru, S., Gedam, S.S., Chander, S. and Sahay, A., 2023. Development of chlorophyll-a concentration estimation algorithm for turbid productive inland waters in India. Geocarto International, 24, pp. 2171143. https://doi.org/10.1080/10106049.2023.2171143

Kumar, S., Arya, S. and Jain, K., 2022. A SWIR-based vegetation index for change detection in land cover using multi-temporal Landsat satellite dataset. International Journal of Information Technology, 14, pp. 2035–2048. https://doi.org/10.1007/s41870-021-00797-6

Liu, R., Chen, J.M., Liu, J., Deng, F. and Sun, R., 2007. Application of a new leaf area index algorithm to China's landmass using MODIS data for carbon cycle research. Journal of Environmental Management, 85(3), pp. 649–658. https://doi.org/10.1016/j.jenvman.2006.04.023

Ma, Z.G., Chen, M.X., Quan, W., PingHeng, L. and Jiapaer, G., 2012. Retrieval of leaf biochemical properties by inverse PROSPECT model and hyperspectral indices: an application to Populus euphratica polymorphic leaves. Spectroscopy and Spectral Analysis, 32(1), pp. 52–62. https://doi.org/10.3724/SP.J.1227.2012.00052

Murugan, P., Sivakumar, R., Pandiyan, R. and Annadurai, M., 2016. Comparison of in-situ hyperspectral and Landsat ETM+ data for chlorophyll-a mapping in case-II water (Krishnarajapuram Lake, Bangalore). Journal of the Indian Society of Remote Sensing, 44, pp. 949–957. https://doi.org/10.1007/s12524-015-0531-8

Nagler, P.L., Scott, R.L., Westenburg, C., Cleverly, J.R., Glenn, E.P. and Huete, A.R., 2005. Evapotranspiration on western US rivers estimated using the enhanced vegetation index from MODIS and data from eddy covariance and Bowen ratio flux towers. Remote Sensing of Environment, 97(3), pp. 337–351. https://doi.org/10.1016/j.rse.2005.05.011

Pandey, S.K.K. and Singh, H., 2011. A simple, cost-effective method for leaf area estimation. Journal of Botany, 1, pp. 658240. https://doi.org/10.1155/2011/658240

Pei, F., Wu, C., Liu, X., Li, X., Yang, K., Zhou, Y. and Xia, G., 2018. Monitoring the vegetation activity in China using vegetation health indices. Agricultural and Forest Meteorology, 248, pp. 215–227. https://doi.org/10.1016/j.agrformet.2017.10.001

Qi, J., Kerr, Y.H., Moran, M.S., Weltz, M., Huete, A.R., Sorooshian, S. and Bryant, R., 2000. Leaf area index estimates using remotely sensed data and BRDF models in a semiarid region. Remote Sensing of Environment, 73(1), pp. 18–30. https://doi.org/10.1016/S0034-4257(99)00113-3

Rouse, J.W., Haas, R.H., Deering, D.W., Schell, J.A. and Harlan, J.C., 1974. Monitoring the vernal advancement and retrogradation (green wave effect) of natural vegetation. NASA Publication, No. E75-10354.

Sebastiani, A., Salvati, R., and Manes, F., 2023. Comparing leaf area index estimates in a Mediterranean forest using field measurements, Landsat 8, and Sentinel-2 data. Ecological Processes, 12(1), pp. 15–28. https://doi.org/10.1186/s13717-023-00441-0

Solgi, E., Soleimany, A. and Hatami, V., 2023. Zoning of leaf chlorophyll content of tree species (a case study in Malayer City, Iran): An indicator to investigate air pollution in urban environments. Journal of School of Public Health and Institute of Public Health Research, 21(2), pp. 263–278.

Taugourdeau, S., Le Maire, G., Avelino, J., Jones, J.R., Ramirez, L.G., Quesada, M.J. and Roupsard, O., 2014. Leaf area index as an indicator of ecosystem services and management practices: An application for coffee agroforestry. Agriculture, Ecosystems & Environment, 192, pp. 19–37.

Tsalyuk, M., Kelly, M., Koy, K.W.M., Getz, W. and Butterfield, H.S., 2015. Monitoring the impact of grazing on rangeland conservation easements using MODIS vegetation indices. Rangeland Ecology & Management, 68(2), pp. 173–185. https://doi.org/10.1016/j.rama.2015.01.006

Tucker, C.J., 1979. Red and photographic infrared linear combinations for monitoring vegetation. Remote Sensing of Environment, 8, pp.127–150. https://doi.org/10.1016/0034-4257(79)90013-0

Turner, D.P., Cohen, W.B., Kennedy, R.E., Fassnacht, K.S. and Briggs, J.M., 1999. Relationships between leaf area index and Landsat TM spectral vegetation indices across three temperate zone sites. Remote Sensing of Environment, 70, pp. 52–68. https://doi.org/10.1016/S0034-4257(99)00057-7

Wong, G., Greenhalgh, T., Westhorp, G., Buckingham, J. and Pawson, R., 2013. RAMESES publication standards: realist syntheses. BMC Medicine, 11, pp.1–14.

Yan, G., Hu, R., Luo, J., Weiss, M., Jiang, H., Mu, X., Xie, D. and Zhang, W., 2019. Review of indirect optical measurements of leaf area index: Recent advances, challenges, and perspectives. Agricultural and Forest Meteorology, 265, pp. 390–411. https://doi.org/10.1016/j.agrformet.2018.11.033

10.57647/jrs.2026.1603.23